Journal of Power Sources 244 (2013) 581–585

Contents lists available at SciVerse ScienceDirect

Journal of Power Sources

journal homepage: www.elsevier.com/locate/jpowsour

Short communication

Crystal and local structure studies of $LiFe_{0.48}Mn_{0.48}Mg_{0.04}PO_4$ cathode material for lithium rechargeable batteries

Donghyuk Jang, Kowsalya Palanisamy, Jeongbae Yoon, Yunok Kim, Won-Sub Yoon*

Department of Energy Science, Sungkyunkwan University, Suwon 440-746, Republic of Korea

HIGHLIGHTS

- ► Mg^{2+} substitution causes smaller local structure distortion and disorder during lithium extraction.
- ► Formation of Pseudo one phase reaction favors the lithium ion insertion and structural stability of $LiFe_{0.48}Mn_{0.48}Mg_{0.04}PO_4$.
- ► The smaller lattice mismatch achieved by cation substitution of Mg^{2+} ion in $LiFe_{0.48}Mn_{0.48}Mg_{0.04}PO_4$ system.

ARTICLE INFO

Article history:
Received 21 November 2012
Received in revised form
8 January 2013
Accepted 17 January 2013
Available online 26 January 2013

Keywords:
Lithium-ion battery
Olivine structure cathode
Pseudo one phase reaction
X-ray absorption near edge structure
Extended X-ray absorption fine structure

ABSTRACT

Synchrotron based *in situ* X-ray absorption spectroscopy (XAS) and X-ray diffraction (XRD) techniques are used to investigate changes in the electronic and local structure of $LiFe_{0.48}Mn_{0.48}Mg_{0.04}PO_4$ olivine type cathode material during charge. The Fe and Mn K-edge XANES results show that the major charge compensation is achieved by the oxidation of Fe^{2+} ions at lower potential plateau (~3.5 V) and the oxidation of Mn^{2+} ions at higher potential plateau (~4.1 V). In Fe K-edge EXAFS results, the increase in Fe–O peak intensity during charge indicates the decrease in the degree of structural disorder around Fe ions. Pseudo one phase reaction is observed during charge, which is consistent with the local structural behavior around Fe ions. Trace amount of Mg^{2+} ion decreases the lattice misfit at the phase boundary during Li extraction. The smaller lattice mismatch near the phase boundary facilitates the conversion of one phase to another resulting in less polarization and better rate capability of electrode.

1. Introduction

Lithium metal phosphates ($LiMPO_4$) with ordered olivine structure have been spotlighted as promising cathode materials for lithium rechargeable batteries. The strong P–O bond in orthorhombic lattice makes the olivine structure reasonably more stable than layered and spinel type material. The practical capacity of olivine $LiFePO_4$ cathode material is close to its theoretical value (168 $mAhg^{-1}$). Structural similarity between charged and discharged states of iron phosphate structure not only possesses a good cycle life but also shows excellent safety characteristics when the battery is fully charged. In recent years, there is an increasing interest in olivine structured materials such as $LiMnPO_4$, $LiNiPO_4$ and $LiCoPO_4$ due to their higher chemical potentials compared to $LiFePO_4$. Among the above mentioned materials, structural stability and electrochemical performance of $LiMnPO_4$ match with those of $LiFePO_4$ [1–8].

Crystal structure of $LiMPO_4$ has an orthorhombic unit cell ($\sim D_{2h}^{16}$–$Pmnb$), which accommodates four units of $LiMPO_4$. In phospho olivine compounds, lithium and transition metal ions occupy the 4a and 4c octahedral sites and the oxygen ions are arranged in hexagonal close packed structure. Metal atoms occupy the zigzag chain of corner-shared octahedra running parallel to *c* axis in the alternate *a*–*c* planes. These chains are bridged by corner and edge-shared (PO_4^{3-}) polyanions to form a host structure with a strong three dimensional bonding. Li ions in olivine structure form LiO_6 octahedra which share the corners along *b* axis. These corner-sharing octahedra are separated by vacant tetrahedral and no atom separates Li ion in adjacent site along this direction to screen the electrostatic interaction. Hence, the movement of Li ion is correlated in one-dimensional channel [1,8].

Several hypotheses state that $LiMnPO_4$ material undergoes poor lithium diffusion kinetics due to lower ionic and electronic conductivity and that Jahn–Teller distortion of Mn^{3+} ions and large volume changes between $LiMnPO_4$ and $MnPO_4$ cause large interface strain [6]. On the other hand, $LiMnPO_4$ has higher energy density than $LiFePO_4$ due to its higher chemical potential of

* Corresponding author. Tel.: +82 31 299 6276; fax: +82 31 299 4279.
E-mail address: wsyoon@skku.edu (W.-S. Yoon).

0378-7753/$ – see front matter © 2013 Elsevier B.V. All rights reserved.
http://dx.doi.org/10.1016/j.jpowsour.2013.01.108

Mn^{2+}/Mn^{3+} (4.1 V) redox couple [9]. To overcome the limitations of individual metal phosphate, multi component systems have been proposed, where transition metal ions are combined in an effective way to form a homogenous solid solution phase [1,2,10]. $LiFe_{1-y}Mn_yPO_4$ is considered as one of the most promising binary cathode materials because of its favorable operating voltages between 3.5 and 4.2 V. Yamada et al. reported that $Li(Mn_yFe_{1-y})PO_4$ materials show better kinetic and utilization properties than pure $LiMnPO_4$ electrode material [7].

Divalent cation substitution such as Mg^{2+}, Zn^{2+}, Cu^{2+}, Ni^{2+}, and Co^{2+} in the metal site significantly improves the electronic conductivity and mobility of Li ions in $LiMPO_4$ material [6,11,12]. Hence, clear understanding of the role of cation substitution in multi-component olivine system is crucial for the advancement of cathode material. Here, we report the bulk and local structure behavior of $LiFe_{0.48}Mn_{0.48}Mg_{0.04}PO_4$ during electrochemical extraction of Li-ions by using synchrotron based X-ray absorption and diffraction techniques.

2. Experimental

$LiFe_{0.48}Mn_{0.48}Mg_{0.04}PO_4$ electrodes were provided by UMICORE. For the *in situ* XRD and XAS test, the cathodes were incorporated into *in situ* cells with a metallic Li foil negative electrode and a Celgard separator. The electrolytes used were commercially available 1 M $LiPF_6$ in a 1:1 EC: DMC solvent. XAS measurements were performed in transmission mode at beamline 8C at Pohang Light Source (PLS-II) using a Si (111) double-crystal monochromator detuned to 80% of its original intensity in order to eliminate the high order harmonics. The storage ring was operated with electron energy of 2.5 GeV and a current between 80 and 120 mA. Reference spectrum of each element was simultaneously collected with the corresponding spectrum of the *in situ* cells using Mn and Fe reference foils. The *in situ* XRD patterns were collected at beamline 1D using a Mar 345-image plate detector with the wavelength of 1.0331 Å. For easy comparison, 2θ of all XRD patterns were recalculated and converted to the corresponding angles for $k = 1.54$ Å (Cu-Kα radiation).

EXAFS data analysis was carried out using standard procedures as described in elsewhere [13]. The measured absorption spectrum below the pre-edge region was fitted to a straight line. The background contribution above the post-edge region, $\mu_0(E)$ was fitted to a fourth order polynomial (cubic spline). The fitted polynomials were extrapolated through the total energy region and subtracted from the total absorption spectra. The background subtracted absorption spectra were normalized for the above energy region $\chi(E) = \{(\mu(E) - \mu_0(E)\}/\mu_0(E)$. The normalized $\chi(E)$ spectra were converted to $\chi(k)$ in k space, where $k = [8\pi^2 m(E - E_o)/h^2]^{1/2}$. The $\chi(k)$ spectra were k^3-weighted to magnify the small signal in the higher k space. The normalized k^3-weighted EXAFS spectra, $k^3\chi(k)$, were Fourier transformed (FT) in k space with integration limits of 3.0–11.0 Å^{-1} for Mn and Fe in order to show the contribution of each bond pair. The experimental Fourier fitted $k^3\chi(k)$ spectra were obtained from the inverse transformation with the hanging window function in k space range between 1.0 and 3.0 Å.

3. Results and discussion

First charge profile during *in situ* XAS characterization of $LiFe_{0.48}Mn_{0.48}Mg_{0.04}PO_4$ cathode is shown in Fig. 1. Two distinct voltage plateaus corresponding to the electrochemical reaction of Fe and Mn ions were observed. First voltage plateau corresponds to redox potential of Fe^{2+}/Fe^{3+} (~3.5 V) and second voltage plateau corresponds to redox potential of Mn^{2+}/Mn^{3+} (~4.1 V). This result

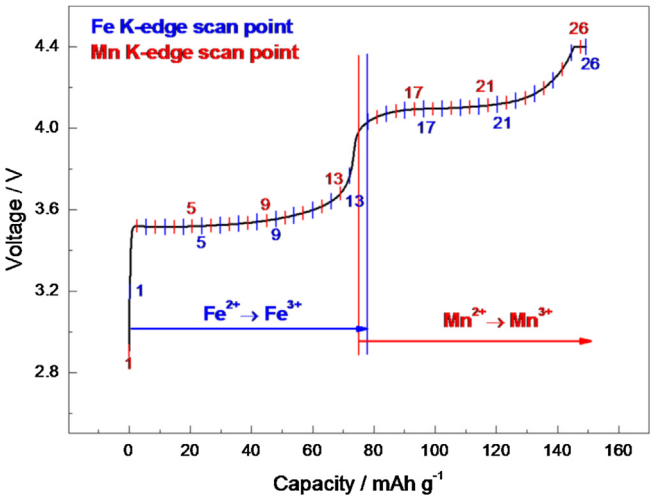

Fig. 1. First charge curves of $LiFe_{0.48}Mn_{0.48}Mg_{0.04}PO_4$ electrode.

is in good agreement with previous results of $Li_{1-x}Mn_{0.5}Fe_{0.5}PO_4$ cathode material [1,4].

Fig. 2(a) and (b) represent *in situ* Fe and Mn K-edge X-ray absorption near edge (XANES) spectra of $LiFe_{0.48}Mn_{0.48}Mg_{0.04}PO_4$

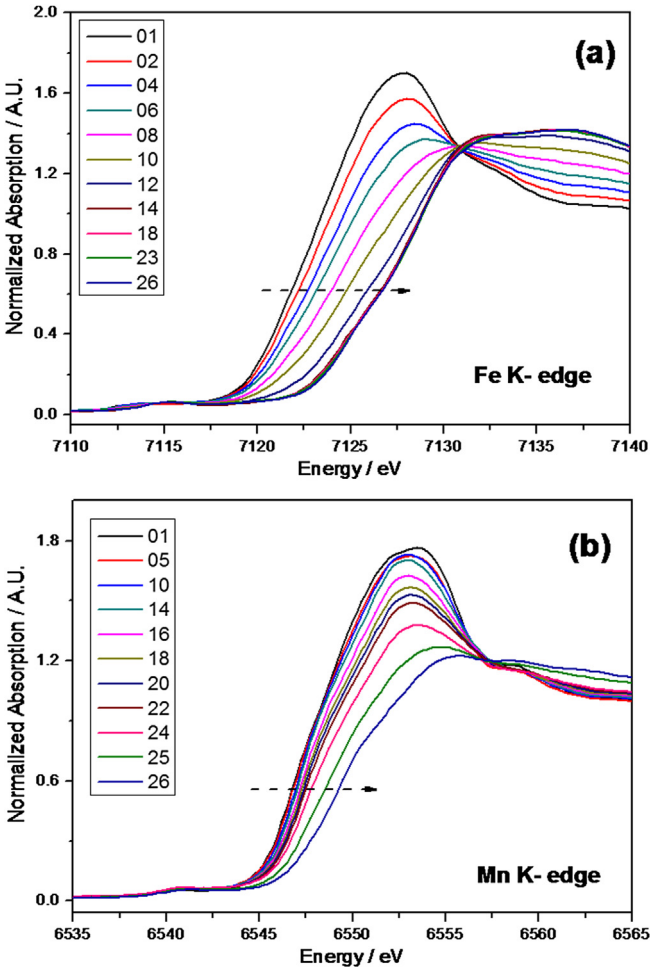

Fig. 2. The normalized *in situ* XANES spectra for (a) Fe and (b) Mn K-edges during first charge.